Comparative Investigation of the LOV1 and LOV2 Domains in *Adiantum* Phytochrome3†

Tatsuya Iwata,‡ Dai Nozaki,‡ Satoru Tokutomi,§ and Hideki Kandori*,‡

Department of Materials Science and Engineering, Nagoya Institute of Technology, Showa-ku, Nagoya 466-8555, Japan, and Research Institute for Advanced Science and Technology, University of Osaka Prefecture, Sakai, Osaka 599-8570, Japan

Received December 27, 2004; Revised Manuscript Received March 14, 2005

ABSTRACT: Phototropin (phot) is a blue-light photoreceptor for phototropic responses, relocation of chloroplasts, and stomata opening in plants. Phototropin has two chromophore-binding domains named LOV1 and LOV2 in its N-terminal half, each of which binds a flavin mononucleotide (FMN) noncovalently. The C-terminal half is a Ser/Thr kinase. A transgenic study of *Arabidopsis* suggested that only LOV2 domain is necessary for the kinase activity, whereas X-ray crystallographic structures of LOV1 and LOV2 domains are almost identical. These facts imply that the detailed structures and/or structural changes are different between LOV1 and LOV2 domains. In this study, we compared light-induced structural changes of the LOV1 and LOV2 domains of a phototropin, *Adiantum* phytochrome3 (phy3), by means of UV−visible and Fourier transform infrared (FTIR) spectroscopy. Photochemical properties of an adduct formation between FMN and a cysteine are essentially similar between phy3-LOV1 and phy3-LOV2. On the other hand, the S−H group of the reactive cysteine forms a hydrogen bond in phy3-LOV1, which is strengthened at low temperatures. This is possibly correlated with the fact that no adduct formation takes place for phy3-LOV1 at 77 K as revealed by the UV−visible absorption spectra. The most prominent difference was seen in the amide-I vibration that monitors the secondary structure of peptide backbone. Protein structural changes in phy3-LOV2 involve the regions of loops, α-helices, and β-sheets, which differ significantly among various temperatures. Extended protein structural changes are probably correlated with the signal transduction activity of LOV2. In contrast, protein structural changes were very small in phy3-LOV1, and they were almost temperature independent. The photocycle of phy3-LOV1 takes 3.1 h, being more than 100 times longer than that of phy3-LOV2. These facts suggest that *Adiantum* phy3-LOV1 does not work for light sensing, being consistent with the previous transgenic study of *Arabidopsis*. It is likely that plants utilize a unique protein architecture (LOV domain) for different functions by regulating their protein structural changes.

Phototropin (phot) is a blue-light receptor protein in plants which is involved in phototropism (*1*), chloroplast movement (*2*), and the stomata opening (*3*). Higher plants have two isoforms of phot, phot1, and phot2, which possess different sensitivities to light (*4*). Phot is composed of ∼1000 amino acid residues and two prosthetic FMN[1] molecules. The two FMN binding domains (ca. 100 residues) are named LOV (light-, oxygen-, and voltage-sensing) domains, which are the subset of the PAS (Per−Arnt−Sim) superfamily. In phot, the LOV1 and LOV2 domains are located at the N-terminal half, and the C-terminal half has a Ser/Thr kinase motif. Thus, the photochemical reaction of FMN yields kinase activation through the domain−domain interaction, whereas the mechanism is yet unclear.

LOV domains have characteristic absorptions at about 450 nm, so that they look yellow. Light absorption of FMN leads to formation of a triplet excited state that absorbs at about 660 nm. The intersystem crossing takes place with a time constant of 3 ns in *Adiantum* phy3-LOV2 and oat phot1-LOV2 (*5*). Then, a ground-state intermediate is formed that absorbs at 390 nm (S390 intermediate). It is now known that the reaction is an adduct formation between FMN and a nearby cysteine (*6*−*10*). Adduct formation takes place with a time constant of 4 μs in oat phot2-LOV2 (*8*) and with 0.9 and 4 μs in *Chlamydomonas* phot-LOV1 (*11*). Since S390 is the sole intermediate in the photocycle of LOV domains, it is believed that S390 is the intermediate activating the kinase domain.

One of the interesting questions is why phot has two LOV domains. Previous molecular biological experiments using expression in insect cells and transgenic *Arabidopsis* reported that only the photochemical reaction of LOV2 is necessary for the expression of the kinase activation and that phototropin works even if LOV1 did not respond to the light for both phot1 and phot2 (*12*). This result implies that the LOV2 domain is only functionally important in phot. Quantum efficiencies of the photoreaction were about 10 and 2 times higher in the LOV2 domain than in the LOV1 domain for

† This work was supported in part by grants from Japanese Ministry of Education, Culture, Sports, Science, and Technology (13139205 to S.T. and 14658215 to H.K.) and by the NITECH 21st Century COE Program to T.I.

* To whom correspondence should be addressed. Phone and fax: 81-52-735-5207. E-mail: kandori@nitech.ac.jp.

‡ Nagoya Institute of Technology.

§ University of Osaka Prefecture.

[1] Abbreviations: FMN, flavin mononucleotide; LOV, light−oxygen−voltage; PAS, Per−Arnt−Sim; FTIR, Fourier transform infrared; UV, ultraviolet.

10.1021/bi047281y CCC: $30.25
Published on Web 04/30/2005

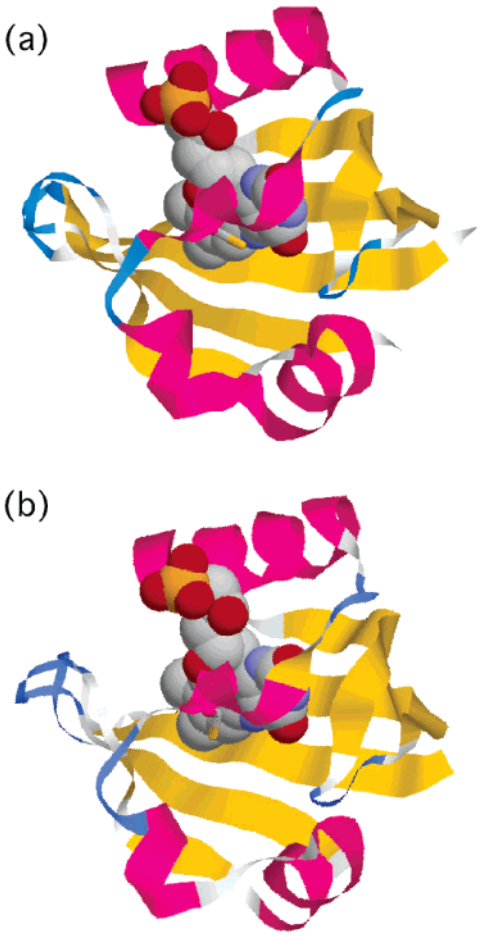

FIGURE 1: Protein structures of (a) *Chlamydomonas* phot-LOV1 (PDB: 1N9N) (*15*) and (b) *Adiantum* phy3-LOV2 (PDB: 1G28) (*14*). The backbone structures of α-helices, turns, and *β*-sheets are colored by red, blue, and yellow, respectively. FMN is shown by space-filling drawings, while the reactive cysteine is shown by stick drawings.

Arabidopsis phot1 and phot2, respectively (*6*, *13*). Higher quantum efficiency of LOV2 is consistent with its functional importance. Nevertheless, recent structural determinations of LOV1 and LOV2 domains provided intriguing results. Crosson and Moffat crystallized the LOV2 domain of *Adiantum* phy3 (*14*), while Fedorov et al. crystallized the LOV1 domain of *Chlamydomonas* phot (*15*) (Figure 1). According to the obtained structures, LOV1 and LOV2 domains were surprisingly similar. This fact suggests that the detailed structures and/or structural changes are different between LOV1 and LOV2 domains.

We have studied structure and structural changes of the LOV2 domain in a phototropin, phytochrome3 (phy3), by means of FTIR spectroscopy. Phy3 is a fusion protein of phot containing the phytochrome chromophoric domain. In the first paper, we showed that the reactive cysteine is protonated in the unphotolyzed state (*16*). Although X-ray crystallography of the S390 intermediate reported very limited structural changes around the FMN chromophore (*10*), we observed the progressive protein structural changes that involve α-helix and *β*-sheet regions (*17*). This observation suggests the presence of global protein structural changes involving the surface of phy3-LOV2. After our FTIR study, global protein changes have been suggested by several spectroscopic studies of LOV domains in solution. Harper et al. reported the presence of α-helix at the C-terminal side of oat phot1-LOV2, and the helix becomes loose upon light absorption by NMR spectroscopy (*18*). By small-angle X-ray scattering, we recently showed that the linker region at the C-terminal side changed relative to the LOV domain in *Arabidopsis* phot1-LOV2 by light illumination, being consistent with the NMR result (*19*). Thus, little structural changes at the surface of phy3-LOV2 in the X-ray crystallographic study may originate from the limited protein motion in the crystal.

We also reported that Gln1029 plays an important role in the protein structural changes of phy3-LOV2 (*20*). Previous X-ray crystallographic studies of phy3-LOV2 found that the N−H group of Gln1029 forms a hydrogen bond with the C(4)═O group of FMN in the unphotolyzed state, while the C═O group of Gln1029 is hydrogen-bonded with the N(5)−H group of FMN in the S390 intermediate (*10*). These observations implied an important structural role of Gln1029 in phy3-LOV2. Our FTIR study indeed showed that the Q1029L mutant protein lacks temperature-dependent protein structural changes involving *β*-sheets, and we concluded that Gln1029 is a key residue in the signal transfer from the chromophore domain to the *β*-sheet at protein surface (*20*). In addition, we recently detected water structural changes in the activation processes of phy3-LOV2 (*17*, *21*). By use of mutant proteins, we concluded that the observed vibrational bands of water monitor the local structural changes near the FMN chromophore (*21*). In this way, we have accumulated spectroscopic data for phy3-LOV2.

In the present study, we aimed at revealing the difference in detailed structures and/or structural changes between the LOV1 and LOV2 domains of phy3. We measured the UV−visible and FTIR spectra of phy3-LOV1 under the same conditions for phy3-LOV2. Although the photochemical properties of adduct formation are essentially similar, we found different protein structural changes between phy3-LOV1 and phy3-LOV2. Protein structural changes in phy3-LOV2 involve the regions of loops, α-helices, and *β*-sheets, which are highly temperature dependent. In contrast, protein structural changes were very small in phy3-LOV1, which was almost temperature independent. The photocycle of phy3-LOV1 was much longer than that of phy3-LOV2, and the correlation between protein structural changes and photocycle kinetics was confirmed by examining the Q1029L mutant of phy3-LOV2. The functional role of LOV1 and LOV2 domains in phot is discussed on the basis of the present results.

MATERIALS AND METHODS

Sample Preparation. The construct containing N-terminal Gly660−Val805 of phy3 was expressed in *Escherichia coli* BL21 (DE3) pLysS cells (Novagen). Overexpression and purification of CBP-phy3-LOV1 were carried out by the same procedure as used for CBP-phy3-LOV2 (*17*). The purified protein was concentrated to give a final concentration of 2.5 mg/mL by using a Microcon YM-10 instrument (Millipore) and dialyzed against 1 mM K/phosphate buffer (pH 7). Then 70−80 *μ*L of the solution was placed on a BaF_2 window, and the dry films were hydrated by dropping H_2O next to the film on the window. Hydration conditions for phy3-LOV1 and phy3-LOV2 were identical.

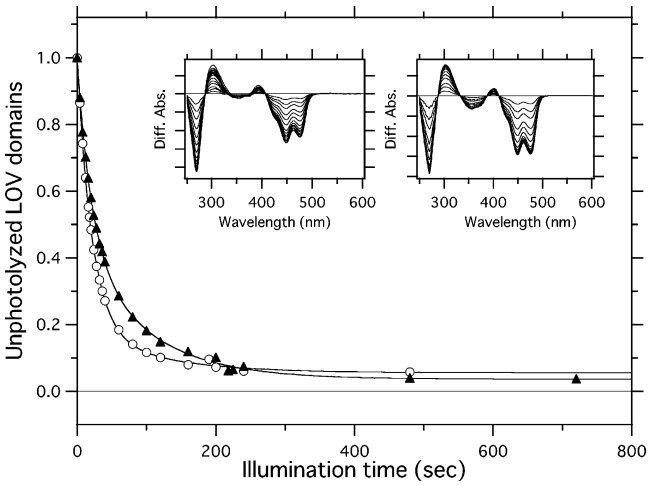

FIGURE 2: Time course of the photoconversion of phy3-LOV1 (closed triangles) and phy3-LOV2 (open circles) to the S390 intermediate measured at 250 K. The *y*-axis corresponds to the remaining unphotolyzed state, which is estimated from the absorbance at 475 nm. Smooth lines are double exponential fitting curves. The insets show the difference spectra of LOV1 (left) and LOV2 (right). The spectra of illumination at 4, 8, 12, 20, 28, 40, 60, 80, 100 120, 160, 200, 240, 480, 720, and 960 s are shown. One division of the *y*-axis corresponds to 0.02 absorbance unit.

Spectroscopy. UV−visible and infrared spectra of the hydrated films were measured using V-550DS (JASCO) and FTS-7000 (Bio-Rad) spectrophotometers, respectively, as described previously (*17*, *20*, *21*). Hydrated films were illuminated by a >400 nm light, which was supplied with a combination of a halogen−tungsten lamp (1000 W) and a long-pass filter (L42, Asahi Techno Glass). For the measurements of quantum efficiency, we also used a 25% neutral density filter (ND-25, Asahi Techno Glass).

Photocycle kinetics experiments were performed for the protein solution of phy3-LOV1 and phy3-LOV2 in 50 mM K/phosphate (pH 7). The dark reversion process from S390 to the original state was monitored at 475 nm by using UV-2400PC (Shimadzu).

RESULTS

Quantum Efficiencies in the Photoconversions of Phy3-LOV1 and Phy3-LOV2 to the S390 Intermediates. Before the UV−visible and FTIR spectra were measured, we compared quantum efficiencies in the photoconversions to S390 between the LOV1 and LOV2 domains. The S390 intermediates formed are thermally reverted to the original states at room temperature, whereas we found that S390 is stable at 250 K both for phy3-LOV1 and for phy3-LOV2. Insets of Figure 2 clearly show that both LOV1 and LOV2 domains are converted to S390 dependent on the illumination time at >400 nm. Figure 2 plots the bleached LOV domains versus illumination time, where the decay "rate" has a correlation with the photosensitivity of the photoconversion to S390, namely, adduct formation.

Figure 2 shows that LOV2 is more photosensitive than LOV1. Both time courses could not be fitted by single exponentials. Double exponential fittings provided the following parameters; decay half-times were 14 s (54%) and 64 s (42%) for LOV1, and 15 s (81%) and 73 s (14%) for LOV2. The remaining 4% and 5% are unreactive portions

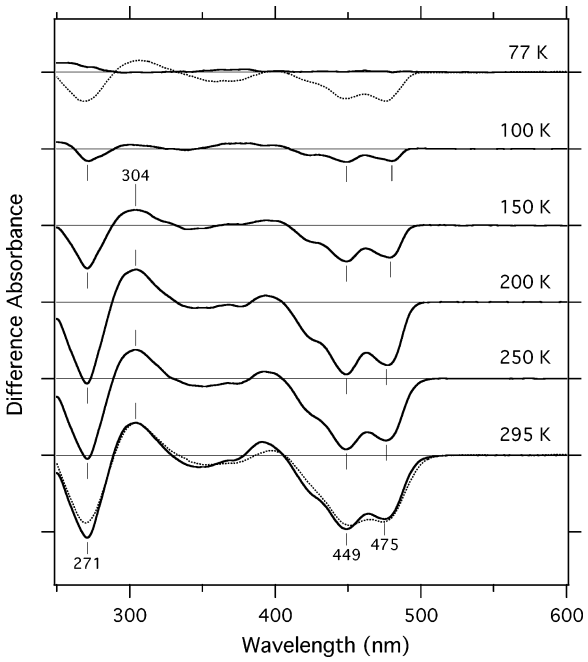

FIGURE 3: Light minus dark difference spectra for phy3-LOV1 (solid line) and phy3-LOV2 (dotted line) in the UV−visible region. The spectra for phy3-LOV2 are reproduced from ref *23*. Spectra are recorded at 77, 100, 150, 200, 250, and 295 K. One division of the *y*-axis corresponds to 0.06 absorbance unit.

for LOV1 and LOV2, respectively. The origin of the fast and slow decays is unclear at present, while similar time constants suggest the common mechanism of photochemistry between LOV1 and LOV2. As the consequence of more populated fast component, LOV2 was more efficiently photoconverted to S390, whose overall difference was about 1.5 times.

Kasahara et al. reported that quantum efficiencies in *Arabidopsis* are 10 times higher in phot1-LOV2 than in phot1-LOV1, whereas the ratio between LOV2 and LOV1 is much smaller for phot2 (*13*). Therefore, *Adiantum* phy3 is phot2-like of *Arabidopsis* in terms of quantum efficiencies of LOV1 and LOV2 domains. This may be correlated with their functions.

Low-Temperature UV−Visible Spectra of Phy3-LOV1 and Phy3-LOV2. Figure 3 shows the difference UV−visible spectra of phy3-LOV1 after and before illumination measured at temperatures from liquid nitrogen to ambient (solid lines). The spectra of phy3-LOV2 at 77 and 295 K are also reproduced from the previous paper (dotted lines) (*17*). The spectra at 295 K are coincident well between the LOV1 and LOV2 domains, being characteristic difference spectra between the S390 and unphotolyzed states. This fact indicates that S390 is formed similarly in phy3-LOV1. Almost identical difference spectra were obtained for LOV1 at lower temperatures such as 250 and 200 K. On the other hand, the amplitude of the spectra is reduced at 150 and 100 K, while spectral shapes are similar. At 77 K, light minus dark spectrum coincides with baseline, indicating no photochemical reaction.

Reduction of the S390 formation at low temperature was also observed for phy3-LOV2 (*17*). Nevertheless, even at 77 K, illumination of phy3-LOV2 yields formation of S390, whose amount is 36% of that at room temperature (dotted lines in Figure 3). Therefore, no adduct formation at 77 K

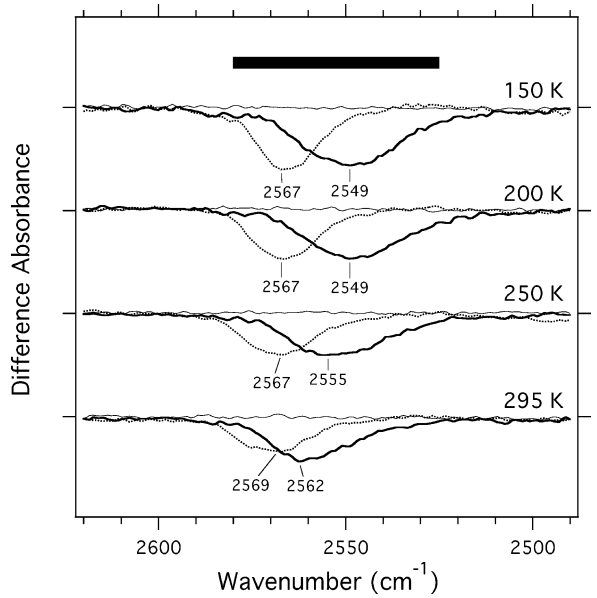

FIGURE 4: Light minus dark (thick solid line) and dark minus dark (thin solid line) infrared difference spectra for phy3-LOV1 in the 2620−2490 cm^{-1} region. Light minus dark difference spectra for phy3-LOV2 are also reproduced from Iwata et al. (dotted line) (*17*). The spectra were recorded at 77, 100, 150, 200, 250, and 295 K. One division of the *y*-axis corresponds to 0.005 absorbance unit. A thick horizontal bar (2580−2525 cm^{-1}) shows the frequency region of the S−H stretch (*16*).

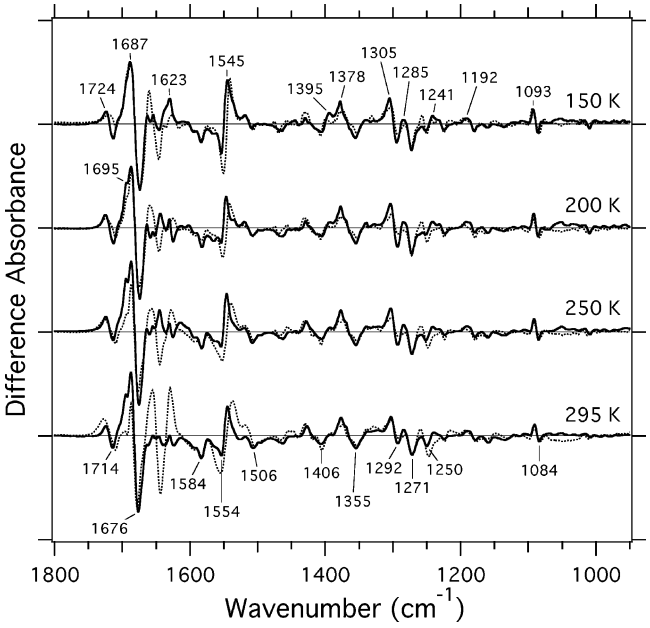

FIGURE 5: Light minus dark infrared spectra for phy3-LOV1 (solid line) in the 1800−950 cm^{-1} region. Light minus dark difference spectra for phy3-LOV2 are also reproduced from Iwata et al. (dotted line) (*17*). The spectra were recorded at 150, 200, 250, and 295 K. One division of the *y*-axis corresponds to 0.0002 absorbance unit. Note that spectra are normalized to show the same photoconversion of the unphotolyzed state to S390 as judged by the UV−visible absorption.

is characteristic for phy3-LOV1. Previously, we discussed that the presence of a nonreactive fraction may originate from the structural heterogeneity between FMN and the cysteine S−H group, and some protein molecules are frozen so that the distance is too far to form an adduct at 77 K (*17*). If this hypothesis is true, the population in the farther distance between FMN and the cysteine S−H group may be larger in LOV1 than in LOV2.

Low-Temperature FTIR Spectra of Phy3-LOV1 and Phy3-LOV2 in the S−H Stretching Region. Figure 4 shows difference IR spectra in the 2620−2490 cm^{-1} region from 150 to 295 K. These spectra are normalized using UV−visible spectra to show the same photoconversion of the unphotolyzed to the S390 state. In the case of phy3-LOV2 (dotted lines), a negative peak was observed at 2567−2569 cm^{-1}, whose temperature dependence was little (*17*). In the case of phy3-LOV1 (thick solid lines), a single negative peak was observed at all the temperatures measured. It is noted that phy3-LOV1 possesses two cysteines at position 712 and 740, where Cys712 corresponds to Cys966 of phy3-LOV2. Nevertheless, observation of a negative band and no corresponding positive band strongly suggests that the adduct formation of Cys712 was only monitored in the spectra, as is for phy3-LOV2. In fact, Thr993 of phy3-LOV2, the corresponding amino acid of Cys740, is located at >10 Å from the FMN chromophore according to the crystal structure (*14*).

The S−H stretching vibrations of phy3-LOV1 appear at lower frequencies than those of phy3-LOV2 (dotted lines). In addition, frequencies are highly temperature dependent in phy3-LOV1, varying from 2562 cm^{-1} (295 K) to 2549 cm^{-1} (150 K). Frequencies for the S−H stretch are much narrower than those for the O−H stretch, but the S−H stretch is downshifted as the hydrogen bond is strengthened as well as the O−H stretch. The frequency of phy3-LOV2 at 2569 cm^{-1} at 295 K corresponds to be almost free from a hydrogen bond, which is consistent with the X-ray crystallographic structure of phy3-LOV2 (*14*). In contrast, the S−H group is likely to form a hydrogen bond in phy3-LOV1. The frequency is further lowered at low temperatures, and the frequency at 150 and 200 K (2549 cm^{-1}) implies a strong hydrogen bond for the S−H group in phy3-LOV1.

The hydrogen-bonding acceptor of the S−H group in phy3-LOV1 is of interest. One of the candidates could be the N(5) atom of FMN. If this is the case, however, lack of adduct formation at low temperatures may be difficult to explain. Therefore, it is likely that the hydrogen-bonding acceptor of the S−H group is some amino acid residues, peptide carbonyls, or internal water molecules. This observation strongly suggests the different local environment of FMN and the reactive cysteine between the LOV1 and LOV2 domains in phy3.

Low-Temperature FTIR Spectra of Phy3-LOV1 in the 1800−950 cm^{-1} Region. Figure 5 compares light minus dark difference IR spectra of phy3-LOV1 (solid line) with those of phy3-LOV2 (dotted line) in the 1800−950 cm^{-1} region at 150−295 K. In the 1600−950 cm^{-1} region, both solid and dotted lines coincide well at each temperature. Both spectra have common positive bands at 1395, 1378, 1305, 1285, 1241, 1192, and 1093 cm^{-1} and negative bands at 1584, 1554, 1506, 1406, 1355, 1292, 1271, 1250, and 1084 cm^{-1}. Many of these bands originate from the FMN chromophore, indicating that the structure and structural changes of FMN are similar between the LOV1 and LOV2 domains.

On the other hand, a highly different spectral feature was obtained in the 1650−1600 cm^{-1} region, which represents characteristic frequencies of amide-I vibrations, C═O stretches of peptide backbone. The C═O stretching vibrations of the

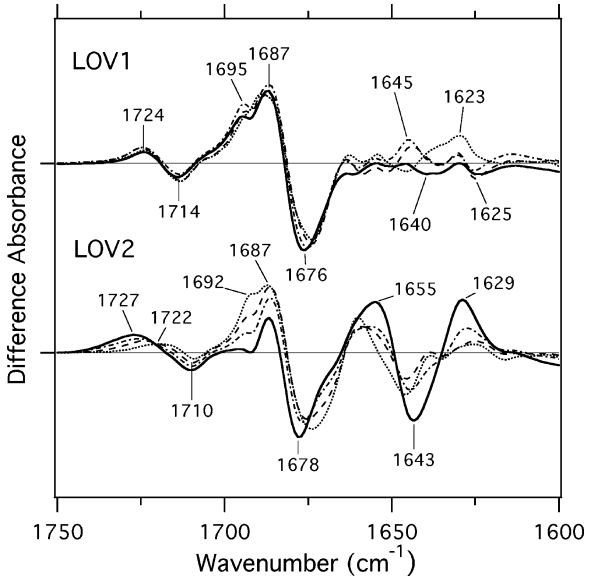

FIGURE 6: Light minus dark infrared spectra for phy3-LOV1 (upper spectra) and phy3-LOV2 (lower spectra) in the 1750−1600 cm^{-1} region. Spectra are measured at 150 (dotted line), 200 (broken line), 250 (dash−dotted line), and 295 K (solid line). One division of the *y*-axis corresponds to 0.008 absorbance unit.

FMN chromophore also appear at about 1710 and 1670 cm^{-1} (C(4)═O and C(2)═O stretches, respectively). Figure 6 highlights the frequency region of amide-I for LOV1 and LOV2 separately. The spectra of LOV2 are highly different among various temperatures. The positive 1692 cm^{-1} band at 150 K disappears at higher temperatures such as 295 K, while a strong positive band at 1629 cm^{-1} appears at 295 K. We interpreted the positive bands at 1692 and 1629 cm^{-1} originating from the structures of turn and β-sheet, respectively (*17*). Thus, temperature-dependent secondary structural alterations in S390 are characteristic of phy3-LOV2.

The spectrum of LOV1 at 150 K (dotted line) has peaks at 1724 (+), 1714 (−), 1695 (+), 1687 (+), 1676 (−), and 1623 (+) cm^{-1}. The peak pair at 1724 (+)/1714 (−) cm^{-1} probably originates from the C(4)═O stretch of FMN. The corresponding negative peak of LOV2 is at 1710 cm^{-1}, indicating that the hydrogen bond of the C(4)═O group is slightly weaker in LOV1 than in LOV2. Similar upshifts to 1724 and 1722 cm^{-1} in LOV1 and LOV2, respectively, after the formation of S390 further imply the common structural changes. The bands at 1695 (+), 1687 (+), and 1676 (−) cm^{-1} are attributable to the amide-I vibrations of the turn structure and C(2)═O stretch. Appearance of a positive peak at 1623 cm^{-1} may suggest the formation of β-sheet-like structure at 150 K. In summary, the spectra at 150 K are similar between the LOV1 and LOV2 domains (Figures 4 and 5).

Figure 6 shows that the spectra of phy3-LOV1 do not change with temperature, unlike phy3-LOV2. The spectrum at 295 K is almost identical to that at 150 K at >1650 cm^{-1}. In the 1650−1600 cm^{-1} region, the spectrum at 295 K is coincident with the baseline. The absence of bands at about 1650 and 1630 cm^{-1} strongly suggests that the formation of S390 does not accompany secondary structural alterations of α-helix and β-sheet, respectively, in phy3-LOV1. Although the bands at 1695 (+), 1687 (+), and 1676 (−) cm^{-1} at 295 K could originate from amide-I vibrations of the turn structure, they could be explained only by the frequency

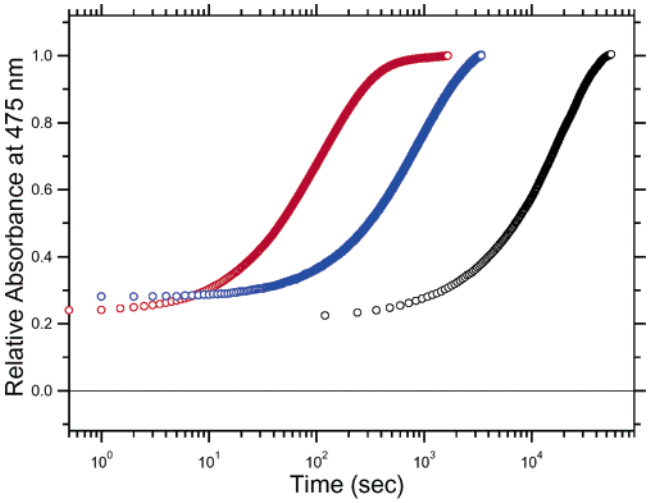

FIGURE 7: Time course of the dark recoveries of phy3-LOV1 (red), the wild-type phy3-LOV2 (black), and the Q1029L mutant phy3-LOV2 (blue) measured at room temperature. Absorptions at 475 nm in the unphotolyzed state are normalized as 1.

changes of the C(2)═O stretch of FMN. Previously, Ataka et al. reported the FTIR spectra of *Chlamydomonas* phot-LOV1, and they concluded that the spectral changes in the amide-I region originate solely from the chromophore vibrations, mainly the C(2)═O stretch of FMN (*22*). We conclude that protein structural changes are much smaller in phy3-LOV1 than in phy3-LOV2.

We previously reported the FTIR spectra of the Q1029L mutant of phy3-LOV2. This mutant lacks temperature-dependent protein structural changes that are characteristic of phy3-LOV2 (*17*). Interestingly, the FTIR spectra of phy3-LOV1 are similar to those of the Q1029L mutant of phy3-LOV2. It is noted that phy3-LOV1 contains the corresponding glutamine (Gln776). Therefore, the present results may suggest the different role of the amino acid residue.

Thermal Reversion of S390 to the Original State. Figure 7 shows the dark reversion processes from the S390 intermediate to LOV1 or LOV2 by monitoring the absorption at 475 nm. They were measured for the LOV domains in solution at 295 K. The kinetics for phy3-LOV1 (black), phy3-LOV2 (red), and the Q1029L mutant protein of phy3-LOV2 (blue) were fitted by single exponentials. The half-lifetimes ($t_{1/2}$) were 90 s for LOV2 and 3.1 h for LOV1. The lifetime of S390 in phy3-LOV1 is the longest among the photocycling LOV domains. The stable S390 state in phy3-LOV1 may be inconvenient for the signal transduction, because it will keep activating the kinase domain for hours even after light is turned off. That is especially the case requiring rapid responses such as chloroplast movements and stomata opening.

It is of interest that the photocycle kinetics are more than 100 times slower for LOV1 than for LOV2, though the adduct formation commonly takes place. An insight can be given by the results in Figure 6, where protein structural changes are very limited for phy3-LOV1. It seems likely that the S390 state exhibiting tiny protein structural changes is long-lived. To further test this possibility, we measured thermal reversion of the Q1029L mutant of phy3-LOV2, because the protein is LOV2, but the protein structural changes are highly limited (*20*). The half-lifetime of S390 of Q1029L was 650 s, being 7.2 times longer than that of

the wild-type phy3-LOV2 (blue curve in Figure 7). Its lifetime is still shorter than that of phy3-LOV1, but a single mutation at position 1029 yields a longer photocycle for phy3-LOV2. Thus, we concluded that the progressive protein structural changes observed for phy3-LOV2 are important not only for the activation of the kinase domain but also for controlling the photocycle kinetics.

DISCUSSION

Difference in the Structure of the Reactive Cysteine and the Adduct Formation Reaction between LOV1 and LOV2. In this paper, we studied difference in photoreactions between the LOV1 and LOV2 domains in *Adiantum* phytochrome3 using low-temperature UV−visible and FTIR absorption spectroscopy. Like phy3-LOV2, only S390 was observed as a stable intermediate of phy3-LOV1. Formation of S390 was reduced at low temperatures for both LOV1 and LOV2 domains. Nevertheless, no formation of S390 was observed at 77 K for phy3-LOV1 (Figure 3). Difference in the local structure around the reactive cysteine presumably influences the specificity in phy3-LOV1. In fact, the hydrogen bond of the cysteine was different between the LOV1 and LOV2 domains. The cysteine S−H group forms a hydrogen bond in phy3-LOV1, which is strengthened at low temperatures.

Recently, Heberle and co-workers reported the FTIR difference spectra in the photoreactions of*Chlamydomonas* phot LOV1, LOV2, and *Bacillus* YtvA LOV at room temperature (*22*, *23*). Negative peaks due to the S−H stretching vibrations were observed at about 2570 cm^{-1} in all cases. Together with our observation for *Adiantum*, it is likely that the protonated S−H group is present in a hydrophobic pocket without a hydrogen bond. In various LOV domains, only phy3-LOV1 possesses a weakly hydrogen-bonded S−H group (2562 cm^{-1}) at room temperature, which is much strengthened at low temperatures.

Partial adduct formation at low temperatures could be explained by structural heterogeneity of proteins (Figure 2). At low temperatures, where the protein structure is frozen, the adduct formation strongly depends on the distance between FMN and the cysteine S−H group. If the distance and orientation of the S−H group are not favorable for the adduct formation at low temperatures, S390 could not be formed. Such multiple conformations may be correlated with the nonexponential feature of the photosensitivity of the S390 formation. In fact, Fedorov et al. showed the two S−H conformations in the crystal structure of *Chlamydomonas* phot-LOV1 at cryogenic temperature (*15*).

Difference in the Protein Structural Changes between LOV1 and LOV2. While the frequency of the S−H stretch is temperature-dependent, the C(4)═O stretch of FMN is temperature-independent for phy3-LOV1 (Figure 6). In the case of phy3-LOV2, the C(4)═O stretch of FMN is temperature-independent for the unphotolyzed state (1710 cm^{-1}), but highly temperature-dependent for the S390 intermediate. The C(4)═O stretch in S390 shifts from 1722 cm^{-1} at 150 K to 1727 cm^{-1} at 295 K (Figure 6). This change is presumably correlated with the temperature-dependent protein structural changes for phy3-LOV2. Such temperature dependence of the C(4)═O stretch in phy3-LOV2 diminishes in the Q1029L mutant (*20*).

In phy3-LOV1, protein structural changes are much smaller than in phy3-LOV2. We infer that the surface structure of phy3-LOV1 is not altered upon formation of S390, because of the lack of the secondary structural alterations. In contrast, phy3-LOV2 exhibits temperature-dependent protein structural changes, suggesting that the surface structure is somehow altered during the appearance of S390. The present observation for each LOV1 and LOV2 molecule is well consistent with the functional importance of the LOV2 domain in the previous molecular biological study (*12*).

Then, a question is raised why protein structural changes are different between phy3-LOV1 and phy3-LOV2. Although we have no clear answer at this moment, our previous study on the Q1029L mutant of phy3-LOV2 may give a hint. By introducing the point mutation at position 1029, we converted the LOV2 domain to the LOV1-like character, exhibiting very small protein structural changes (*20*). Previous X-ray crystallographic studies of phy3-LOV2 showed that the N−H group of Gln1029 forms a hydrogen bond with the C(4)═O group of FMN in the unphotolyzed state (*14*), while the C═O group of Gln1029 is hydrogen-bonded with the N(5)−H group of FMN in the S390 intermediate (*10*). These observations implied an important role of the switch of the hydrogen bond of Gln1029, and our FTIR study indeed showed that the Q1029L mutant protein lacks temperature-dependent protein structural changes involving the β-sheet (*20*). Thus, there must be important structural factors on the intramolecular signal transduction that corresponds to the specific protein structural changes.

It is noted that phy3-LOV1 also possesses the corresponding glutamine at position 776 (Gln776 of phy3-LOV1). This may suggest the different role between Gln776 of phy3-LOV1 and Gln1029 of phy3-LOV2. One possibility is that, unlike phy3-LOV2, the switch of the hydrogen bond of Gln776 does not take place in phy3-LOV1. Namely, Gln776 possibly forms a hydrogen bond with the C(4)═O group of FMN in the unphotolyzed state, whereas the C═O group of Gln776 cannot be hydrogen-bonded with the N(5)−H group of FMN in the S390 intermediate in phy3-LOV1. Another possibility is that there are different factor(s) for the intramolecular signal transduction from FMN to the β-sheet in phy3-LOV2. Thus, it is important to identify the factor-(s) distinguishing protein structural changes between the LOV1 and LOV2 domains.

Figure 7 shows that phy3-LOV1 possesses much longer photocycle kinetics than phy3-LOV2. It may be puzzling that the protein exhibiting smaller structural changes (phy3-LOV1) has a longer lifetime. However, amide-I vibrations in Figure 6 could provide a hint to interpret the apparent inconsistency. Local structure around the reactive cysteine is presumably changed for phy3-LOV1, which corresponds to the turn structure (Figure 8). Although similar changes were observed at low temperatures for phy3-LOV2, global protein structural changes take place at room temperature involving β-sheet (Figure 8). Therefore, we infer that the S390 state of phy3-LOV1 is in a relatively stable structure accompanying local structural alterations.

Role of the LOV1 Domain. The present study revealed that protein structural changes are much greater in phy3-LOV2 than in phy3-LOV1. Temperature-dependent structural changes in phy3-LOV2 suggest that such progressive changes also take place at room temperature. Global protein structural

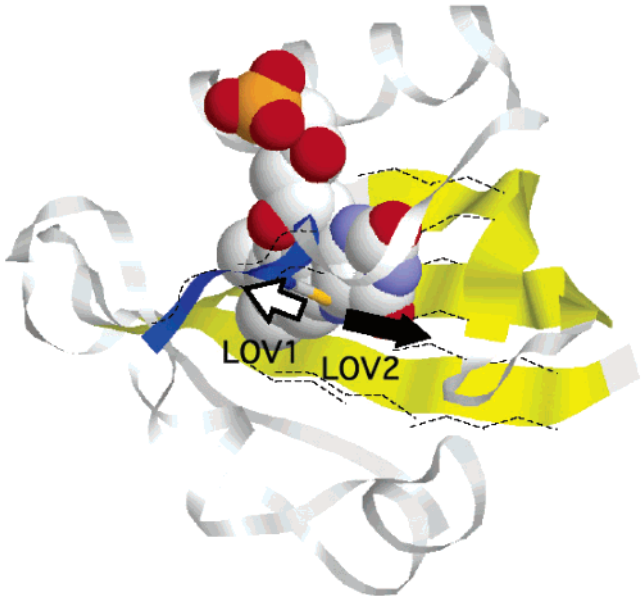

FIGURE 8: Protein structural changes upon formation of S390 are schematically drawn on the LOV-domain structure, where that of *Adiantum* phy3-LOV2 (PDB: 1JUN) (*10*) is shown. The adduct formation between FMN and cysteine causes a conformational change at the β-sheet region in phy3-LOV2 (yellow ribbons), whereas the structural change happens only in the loop region including the cysteine residue in phy3-LOV1 (blue ribbon).

changes must be important for phy3-LOV2 to activate the kinase domain.

The half time-constant of the recovery to the original state was 3.1 h for phy3-LOV1 (Figure 7). In general, the response time to light is longer in plants than in animals and bacteria, the latter of which need quick movements for their survivals. In fact, the deactivation times of light sensor proteins are in the range from milliseconds to seconds in animals and bacteria, such as visual rhodopsin, archaeal sensory rhodopsins, and photoactive yellow proteins (*25*−*27*). Even if phy3-LOV1 acts as a light sensor in *Adiantum*, its photocycle of hours would be too long. Lifetimes of S390 in LOV2 domains are known to be from 4 s to 180 s (*13*), which is convenient to act as plants' light sensors. It is noted that we discuss only the photocycle of sensor proteins, and interaction with activating or deactivating proteins could change the kinetics. For instance, the activated animal rhodopsin is stabilized by forming a complex with a G-protein transducin, while phosphorylated rhodopsin is quickly deactivated by visual arrestin (*28*, *29*). However, photocycle kinetics of sensor proteins themselves probably provide a background of the actual kinetics in cells. The long lifetime of S390 in phy3-LOV1 suggests a different functional role.

Then, what is the role of phy3-LOV1? The recent gel chromatography experiment showed that oat phot1-LOV1 forms homodimer while LOV2 was monomeric in solution (*24*). We showed that *Arabidopsis* phot1-LOV1, phot2-LOV1, and phot2-LOV2 are homodimers, while phot2-LOV2 exists as monomeric forms by using small-angle X-ray scattering (*19*). These observations suggest that the LOV1 domain plays a structural role rather than acting as light sensors. Since LOV domains belong to the PAS domain superfamily, dimer formation of the LOV1 domain is reasonable, and possibly contributing the complex structure of phot.

ACKNOWLEDGMENT

We thank Drs. Y. Furutani and D. Matsuoka for their experimental assistance and Ms. M. Kinoshita for her technical assistance.

REFERENCES

1. Liscum, E., and Briggs, W. R. (1995) Mutations in the *NPH1* Locus of *Arabidopsis* Disrupt the Perception of Phototropic Stimuli, *Plant Cell 7*, 473−485.
2. Kagawa, T., Sakai, T., Suetsugu, N., Oikawa, K., Ishiguro, S., Kato, T., Tabata, S., Okada, K., and Wada, M. (2001) *Arabidopsis* NPL1: A Phototropin Homolog Controlling the Chloroplast High-Light Avoidance Response, *Science 291*, 2138−2141.
3. Kinoshita, T., Doi, M., Suetsugu, N., Kagawa, T., Wada, M., and Shimazaki, K. (2001) phot1 and phot2 mediate blue light regulation of stomatal opening, *Nature 414*, 656−660.
4. Sakai, T., Kagawa, T., Kasahara, M., Swartz, T. E., Christie, J. M., and Briggs, W. R., Wada, W., and Okada, K. (2001) *Arabidopsis* nph1 and npl1: Blue light receptors that mediate both phototropism and chloroplast relocation, *Proc. Natl. Acad. Sci. U.S.A. 98*, 6969−6974.
5. Kennis, J. T. M., Crosson, S., Gauden, M., van Stokkum, I. H. M., Moffat, K., and van Grondelle, R. (2003) Primary Reactions of the LOV2 Domain of Phototropin, a Plant Blue-Light Photoreceptor, *Biochemistry 42*, 3385−3392.
6. Salomon, M., Christie, J. M., Knieb, E., Lempert, U., and Briggs, W. R. (2000) Photochemical and Mutational Analysis of the FMN-Binding Domains of the Plant Blue Light Receptor, Phototropin, *Biochemistry 39*, 9401−9410.
7. Miller, S. M., Massey, V., Ballou, D., Williams, C. H., Jr., Distefano, M. D., Moore, M. J., and Walsh, C. T. (1990) Use of a site-directed triple mutant to trap intermediates: Demonstration that the flavin C(4a)-thiol adduct and reduced flavin are kinetically competent intermediates in mercuric ion reductase, *Biochemistry 29*, 2831−2841.
8. Swartz, T. E., Corchnoy, S. B., Christie, J. M., Lewis, J. W., Szundi, I., Briggs, W. R., and Bogomolni, R. A. (2001) The Photocycle of a Flavin-Binding Domain of the Blue Light Photoreceptor Phototropin, *J. Biol. Chem. 276*, 36493−36500.
9. Salomon, M., Eisenreich, W., Dürr, H., Schleicher, E., Knieb, E., Massey, V., Rüdiger, W., Müller, F., Bacher, A., and Richter, G. (2001) An optomechanical transducer in the blue light receptor phototropin from *Avena sativa*, *Proc. Natl. Acad. Sci. U.S.A. 98*, 12357−12361.
10. Crosson, S., and Moffat, K. (2002) Photoexcited Structure of a Plant Photoreceptor Domain Reveals a Light-Driven Molecular Switch, *Plant Cell 14*, 1067−1075.
11. Kottke, T., Heberle, J., Hehn, D., Dick, B., and Hegemann, P. (2003) Phot-LOV1: Photocycle of a Blue-Light Receptor Domain from the Green Alga *Chlamydomonas reinhardtii*, *Biophys. J. 84*, 1192−1201.
12. Christie, J. M., Swartz, T. E., Bogomolni, R. A., and Briggs, W. R. (2002) Phototropin LOV domains exhibit distinct roles in regulating photoreceptor function, *Plant J. 32*, 205−219.
13. Kasahara, M., Swartz, T. E., Olney, M. A., Onodera, A., Mochizuki, N., Fukuzawa, H., Asamizu, E., Tabata, S., Kanegae, H., Takano, M., Christie, J. M. Nagatani, A., and Briggs, W. R. (2002) Photochemical Properties of the Flavin Mononucleotide-Binding Domains of the Phototropins from *Arabidopsis*, Rice, and *Chlamydomonas reinhardtii*, *Plant Physiol. 129*, 762−773.
14. Crosson, S., and Moffat, K. (2001) Structure of a flavin-binding plant photoreceptor domain: Insights into light-mediated signal transduction, *Proc. Natl. Acad. Sci. U.S.A. 98*, 2995−3000.
15. Fedorov, R., Schlichting, I., Hartmann, E., Domratcheva, T., Fuhrmann, M., and Hegemann, P. (2003) Crystal structures and molecular mechanism of a light-induced signaling switch: The Phot-LOV1 domain from *Chlamydomonas reinhardtii*, *Biophys. J. 84*, 2474−2482.
16. Iwata, T., Tokutomi, S., and Kandori, H. (2002) Photoreaction of the Cysteine S-H group in the LOV2 Domain of *Adiantum* Phytochrome3, *J. Am. Chem. Soc. 124*, 11840−11841.
17. Iwata, T., Nozaki, D., Tokutomi, S., Kagawa, T., Wada, M., and Kandori, H. (2003) Light-Induced Structural Changes in the LOV2 Domain of *Adiantum* Phytochrome3 Studied by Low-Temperature FTIR and UV−Visible Spectroscopy, *Biochemistry 42*, 8183−8191.

18. Harper, S. M., Neil, L. C., and Gardner, K. H. (2003) Structural basis of a phototropin light switch, *Science 301*, 1541−1544.
19. Nakasako. M., Iwata, T., Matsuoka, D. and Tokutom, S. (2004) Light-induced structural changes of LOV-domain containing polypeptides from *Arabidopsis* phototropin 1 and 2 studied by small-angle X-ray scattering, *Biochemistry, 43*, 14881−14890.
20. Nozaki, D., Iwata, T., Ishikawa, T., Todo, T., Tokutomi, S., Kandori, H. (2004) Role of Gln1029 in the Photoactivation Processes of the LOV2 Domain in *Adiantum* phytochrome3, *Biochemistry 43*, 8373−8379.
21. Nozaki, D., Iwata, T., Tokutomi, S. and Kandori, H. (2004) Water Structural Changes in the Activation Process of the LOV2 Domain of *Adiantum* Phytochrome3, *J. Mol. Struct. 735/736*, 259−265.
22. Ataka, K., Hegemann, P., and Heberle, J. (2003) Vibrational Spectroscopy of an Algal Phot-LOV1 Domain Probes the Molecular Changes Associated with Blue-Light Reception, *Biophys. J. 84*, 466−474.
23. Bednarz, T., Losi, A., Gartner, W., Hegemann, P., and Heberle, J. (2004) Functional variations among LOV domains as revealed by FT-IR difference spectroscopy, *Photochem. Photobiol. Sci. 3*, 575−579.
24. Salomon, M., Lempert, U., and Rüdiger. W. (2004) Dimerization of the plant photoreceptor phototropin is probably mediated by the LOV1 domain, *FEBS Lett. 572*, 8−10.
25. Yoshizawa, T., and Kandori, H. (1992) in *Progress in retinal research* (Osborne, N., and Chader, G., Eds.) pp 33−35, Oxford, Pergamon Press.
26. Losi, A., Braslavsky, S. E., Gartner, W., and Spudich, J. L. (1999) Time-Resolved Absorption and Photothermal Measurements with Sensory Rhodopsin I from *Halobacterium salinarum*, *Biophys. J. 76*, 2183−2191.
27. Hoff, W. D., van Stokkum, I. H., van Ramesdonk, H. J., van Brederode, M. E., Brouwer, A. M., Fitch, J. C., Meyer, T. E., van Grondelle, R., and Hellingwerf, K. J. (1994) Measurement and global analysis of the absorbance changes in the photocycle of the photoactive yellow protein from *Ectothiorhodospira halophila*, *Biophys. J. 67*, 1691−1705.
28. Gibson, S. K., Parkes, J. H., and Liebman, P. A. (2000) Phosphorylation Modulates the Affinity of Light-Activated Rhodopsin for G Protein and Arrestin, *Biochemistry 39*, 5738−5749.
29. Pulvermüller, A., Schröder, K., Fischer, K., and Hofmann, K. P. (2000) Interactions of Metarhodopsin II: ARRESTIN PEPTIDES COMPETE WITH ARRESTIN AND TRANSDUCIN, *J. Biol. Chem. 275*, 37679−37685.

BI047281Y